This is an open access article published under an ACS AuthorChoice License, which permits copying and redistribution of the article or any adaptations for non-commercial purposes.

Integrated Ternary Bioinspired Nanocomposites *via* Synergistic Toughening of Reduced Graphene Oxide and Double-Walled Carbon Nanotubes

Shanshan Gong,[†,#] Wei Cui,[†,#] Qi Zhang,[†,#] Anyuan Cao,[§] Lei Jiang,[†] and Qunfeng Cheng[*,†,‡]

[†]Key Laboratory of Bio-inspired Smart Interfacial Science and Technology of Ministry of Education, School of Chemistry and Environment, BeiHang University, Beijing 100191, P.R. China, [‡]State Key Laboratory for Modification of Chemical Fibers and Polymer Materials, Donghua University, Shanghai 201620, P.R. China, and [§]Department of Materials Science and Engineering, College of Engineering Peking University, Beijing 100871, P. R. China. [#]These three authors contributed equally to the work.

ABSTRACT With its synergistic toughening effect and hierarchical micro/nanoscale structure, natural nacre sets a "gold standard" for nacre-inspired materials with integrated high strength and toughness. We demonstrated strong and tough ternary bioinspired nanocomposites through synergistic toughening of reduced graphene oxide and double-walled carbon nanotube (DWNT) and covalent bonding. The tensile strength and toughness of this kind of ternary bioinspired nanocomposites reaches 374.1 ± 22.8 MPa and 9.2 ± 0.8 MJ/m^3, which is 2.6 and 3.3 times that of pure reduced graphene oxide film, respectively. Furthermore, this ternary bioinspired nanocomposite has a high conductivity of 394.0 ± 6.8 S/cm and also shows excellent fatigue-resistant properties, which may enable this material to be used in aerospace, flexible energy devices, and artificial muscle. The synergistic building blocks with covalent bonding for constructing ternary bioinspired nanocomposites can serve as the basis of a strategy for the construction of integrated, high-performance, reduced graphene oxide (rGO)-based nanocomposites in the future.

KEYWORDS: integrated · ternary bioinspired nanocomposite · synergistic toughening · graphene oxide · double-walled carbon nanotube

Graphene's extraordinary properties as the strongest and stiffest material ever measured[1] and the best-known electrical conductor[2] could have promising applications in many fields.[3] However, it is a great challenge to assemble graphene microscale nanosheets into macrosize nanocomposites for practical applications. Nacre, the gold standard for biomimicry, provides an excellent example for assembling two-dimensional (2D) nanosheets into high-performance nanocomposites.[4] In fact, the extraordinary properties of natural nacre are attributed to its unique hierarchical micro/nanoscale structure and synergistic toughening effects from 2D aragonite platelets, one-dimensional (1D) nanofibrillar chitin,[5] and interface interactions.[4] Graphene oxide (GO),[6] a derivative of graphene, is one of the best candidates for fabricating bioinspired nanocomposites owing to its many functional groups on the surface.[7] Recently, many reports on GO-based nanocomposites have been reported.[8] For example, Zhang *et al.*[9] demonstrated ultrastrong GO-based materials (tensile strength of 382 MPa) through $\pi-\pi$ interactions with poly(acrylic acid-*co*-(4-acrylamidophenyl) boronic acid) (PAPB) after chemical reduction. An *et al.*[10] realized ultrastiff GO-based materials (storage modulus of 127 GPa) through borate orthoester covalent bonding. Tian *et al.*[11] also reported on ultrahigh modulus GO-based materials (Young's modulus of 103.4 GPa) through covalent bonding between polydopamine (PDA) grafted on GO nanosheets andpoly-(ether imide) (PEI).

However, the conflicts between strength and toughness have commonly existed in binary nanocomposites.[12] Prasad *et al.*[13]

* Address correspondence to cheng@buaa.edu.cn.

Received for review August 21, 2015 and accepted October 15, 2015.

Published online October 15, 2015
10.1021/acsnano.5b05252

© 2015 American Chemical Society

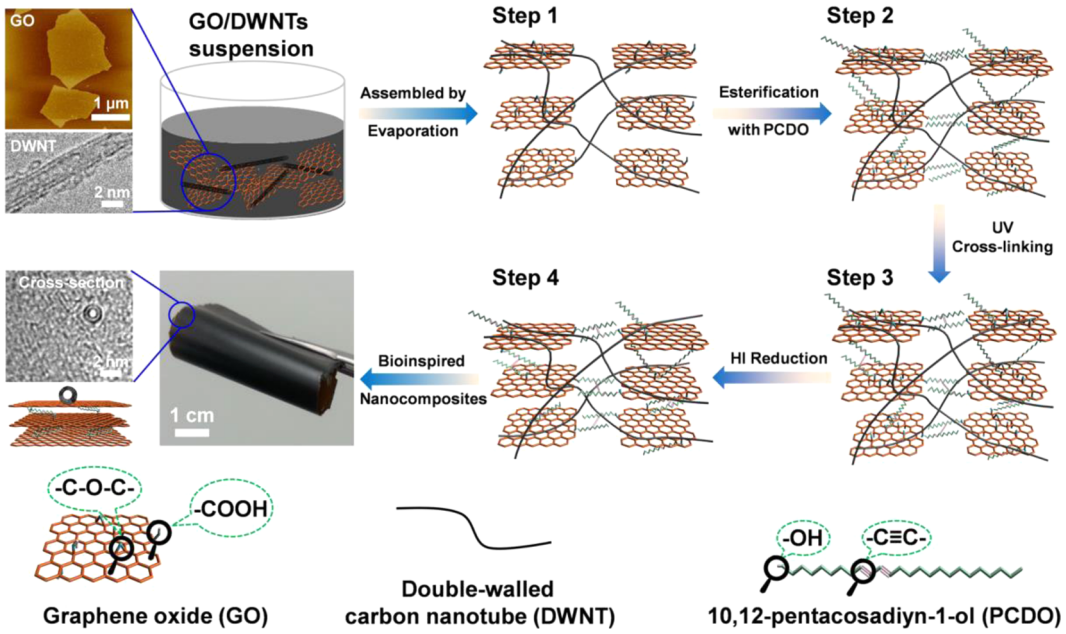

Figure 1. Schematic illustration of process for preparing ternary bioinspired nanocomposites through evaporation self-assembly. Step 1: A suspension of GO/DWNTs was assembled into GO−DWNT hybrid layered materials through an evaporation process. Step 2: The esterification was conducted through immersing the GO−DWNT hybrid layered materials into a PCDO solution. Step 3: The PCDO molecules were cross-linked by 1,4-addition polymerization of their diacetylenic units under UV irradiation. Step 4: ternary bioinspired nanocomposites of rGO−DWNT−PCDO was obtained through HI reduction.

observed the extraordinary synergistic effects in ternary nanocomposites with two different types of nanocarbons incorporated into poly(vinyl alcohol) (PVA). Shin *et al.*[14] achieved ultratough ternary nanocomposite fibers through a synergistic effect from reduced graphene oxide (rGO) and single-walled carbon nanotubes (SWNTs) in the PVA matrix. In our previous work, we also demonstrated an effective synergistic effect and obtained integrated strong and tough ternary bioinspired nanocomposites made of nanoclay/nanofibrillar cellulose/poly(vinyl alcohol)[15] and GO/molybdenum disulfide (MoS_2)/thermoplastic polyurethanes (TPU).[16]

Herein, inspired by the synergistic effect in hierarchical micro/nanoscale of natural nacre, we further demonstrated strong and tough integrated ternary bioinspired nanocomposites through synergistic toughening of graphene oxide (GO) and double-walled carbon nanotube (DWNT) and covalent bonding. The tensile strength and toughness of ternary bioinspired nanocomposites reaches 374.1 ± 22.8 MPa and 9.2 ± 0.8 MJ/m^3, which is 2.6 and 3.3 times that of pure reduced graphene oxide film, respectively. Furthermore, this ternary bioinspired nanocomposite has a high conductivity of 394.0 ± 6.8 S/cm and also shows excellent fatigue-resistant properties, which may enable new materials for use in aerospace, flexible energy devices, and artificial muscle. This strategy of using a synergistic toughening approach opens a new door for constructing high performance, integrated, multifunctional, graphene oxide (GO)-based nanocomposites in the future.

RESULTS AND DISCUSSION

The schematic illustration of the ternary bioinspired nanocomposites fabrication process is shown in Figure 1. In Step 1, the GO/DWNTs homogeneous suspension was first obtained by slowly dropping the DWNT dispersion into GO suspension with continuous stirring and ultrasonication. Then, the GO/DWNTs hybrid building blocks were assembled into GO−DWNT hybrid layered materials through an evaporation process at 45 °C for 2 days. In this work, to explore the synergistic effect, a series of hybrid layered materials with different ratios of GO to DWNT were fabricated, including 70:30 (GO−DWNT-I), 85:15 (GO−DWNT-II), 90:10 (GO−DWNT-III), 93:7 (GO−DWNT-IV), and 95:5 (GO−DWNT-V). The exact contents of GO in the hybrid layered materials were determined by thermogravimetric analysis (TGA), as shown in Figure S1 and Table S1. In Step 2, the GO−DWNT hybrid layered materials were immersed into the 10,12-pentacosadiyn-1-ol (PCDO)/tetrahydrofuran (THF) solution. Esterification between GO and PCDO occurred,[17] which was confirmed by Fourier transform infrared spectroscopy (FTIR) (Figure S2), and X-ray photoelectron spectra (XPS) (Figure S3). In Step 3, 1,4-addition polymerization happened between π-conjugated diacetylenic units on PCDO chains under UV irradiation, forming the covalent cross-linking between adjacent GO nanosheets,[17] leading to the GO−DWNT−PCDO nanocomposites. In Step 4, the residual functional groups on GO nanosheets were removed through chemical reduction of hydroiodic acid (HI), and then the ternary bioinspired nanocomposites

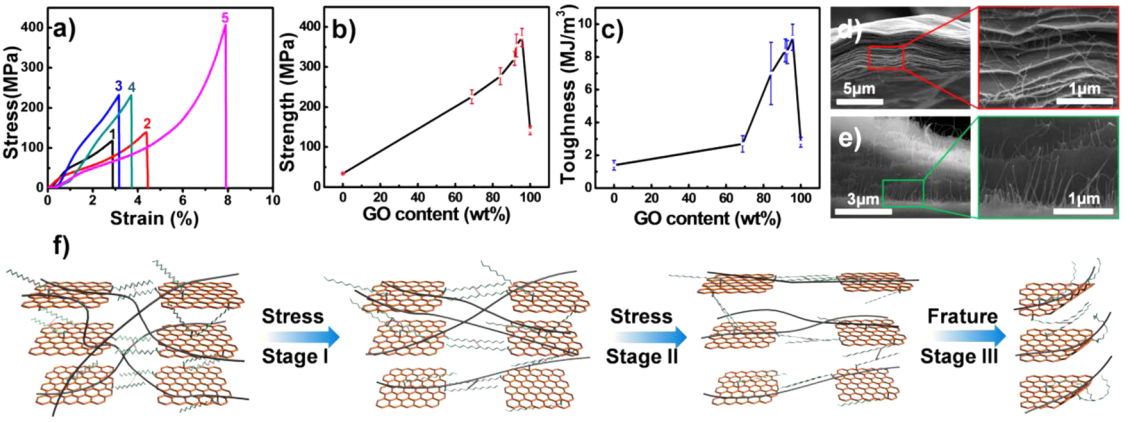

Figure 2. a) Typical strain−stress curves of GO film (curve 1), rGO film (curve 2), GO−DWNT-V hybrid materials (curve 3), GO−DWNT−PCDO-V nanocomposites (curve 4), and rGO−DWNT−PCDO-V nanocomposites (curve 5). (b and c) The strength and toughness of rGO−DWNT−PCDO with different GO contents. (d and e) The front and side view fracture morphology of rGO−DWNT−PCDO-V nanocomposites after tensile testing. (f) The proposed fracture mechanism of rGO−DWNT−PCDO-V nanocomposite under stress.

of rGO−DWNT−PCDO were obtained. X-ray diffraction (XRD) was conducted to further verify the successful introduction of DWNTs and PCDO into the interlayers of GO nanosheets, as shown in Figure S4 and Table S2. The transmission electron microscopy (TEM) image (bottom left) shows the cross-section of ternary bioinspired nanocomposites of rGO−DWNT−PCDO: DWNT is dispersed on the surface of GO nanosheets as proposed in the schematic illustration, which is direct evidence of ternary bioinspired nanocomposites.

Typical stress−strain curves of the prepared samples are shown in Figure 2a. Pure GO film's (curve 1 in Figure 2a) tensile strength (116.5 ± 2.3 MPa) and toughness (1.9 ± 0.1 MJ/m^3) are consistent with a previous report.[18] After the GO film is chemically reduced by HI, the tensile strength and toughness of rGO film (curve 2 in Figure 2a) reach 141.8 ± 10.8 MPa and 2.8 ± 0.3 MJ/m^3, respectively, which is consistent with the previous report.[19] Different ratios of GO to DWNTs result in different synergistic percentages,[13] which play a key role in mechanical properties. With increasing GO contents, the tensile strength and toughness of GO−DWNT hybrid layered materials were dramatically improved, as shown in Figure S5 (the detailed mechanical properties are listed in Table S3). The tensile strength and toughness of GO−DWNT-V hybrid layered materials reach 230.8 ± 3.1 MPa and 3.0 ± 0.3 MJ/m^3 (curve 3 in Figure 2a), respectively. After covalent cross-linking with PCDO, the mechanical properties of rGO and DWNT films were dramatically enhanced. The corresponding tensile stress−strain curves are shown in Figure S6, and the details mechanical properties are listed in Table S3. Especially for ternary bioinspired nanocomposites, for example, the tensile strength and toughness of GO−DWNT−PCDO-V nanocomposites increase to 238.2 ± 5.4 MPa and 4.1 ± 0.4 MJ/m^3 (curve 4 in Figure 2a), respectively. The PCDO content is about 2.24 wt % determined by TGA, as shown in Figure S7. The tensile strength and toughness of rGO−DWNT−PCDO-V further increase up to 374.1 ± 22.8 MPa and 9.2 ± 0.8 MJ/m^3 after HI reduction (curve 5 in Figure 2a), which are 2 and 5 times higher than that of natural nacre (170 MPa and 1.8 MJ/m^3),[20] respectively. Figure 2 panels b and c show that the tensile strength and toughness of rGO−DWNT−PCDO nanocomposites are further improved with increasing GO contents, indicating the synergistic effect from GO nanosheets and DWNTs is enhanced by the covalent bonding between GO nanosheets and PCDO molecules.

The front and side view fracture morphologies of rGO−DWNT−PCDO-V nanocomposites were shown in Figures 2d,e. The GO−DWNT hybrid layered materials show a brittle fractured morphology without the edge curling of GO nanosheets after the DWNTs were pulled out (Figure S8). It is clearly shown that the DWNTs were pulled out along the direction of tensile stretching and the edge of GO nanosheets curled in the rGO−DWNT−PCDO nanocomposites. A typical proposed fracture mechanism is shown in Figure 2f. In the early stretching process of Stage I, the slippage first occurs between adjacent rGO nanosheets, and the DWNTs bridge adjacent rGO nanosheets to resist the sliding, resulting in the stress uniformly dispersing in the rGO nanosheets and DWNTs. For further loading in Stage II, the curly DWNTs and coiled PCDO molecule chains between the rGO nanosheets are gradually stretched along the stretching direction, further absorbing energy. After the π-conjugated force between the rGO nanosheet and DWNTs is broken,[14] the DWNTs were pulled out, resulting in a large plastic deformation. When the loading further increased in Stage III, the covalent bonding between the PCDO and rGO nanosheets is broken, and the external force induces the curling of the edge of the rGO nanosheets.

To quantify the synergistic effect on the mechanical properties' improvement of ternary bioinspired

nanocomposites, the synergy percentage (S) proposed by Prasad[13] is modified as follows:

$$S = \frac{2\sigma_{hyb} - (\sigma_{DWNT} + \sigma_{GO})}{\sigma_{DWNT} + \sigma_{GO}} \times 100$$

where σ_{hyb}, σ_{DWNT}, and σ_{GO} represent the tensile strength of GO–DWNT hybrid layered materials, DWNT film, and GO film, respectively. The synergy percentage of tensile strength for binary GO–DWNT hybrid layered materials and ternary bioinspired nanocomposites are also listed in Table S3. As shown in Figure 3, the synergy percentage dramatically increases with GO contents. For example, the strength synergy percentage increases from 73.6% for GO–DWNT-I to 206.5% for GO–DWNT-V. After covalent cross-linking with PCDO, the synergy percentage is further enhanced, and the strength synergy percentage is enhanced 325.4% for rGO–DWNT–PCDO-V ternary bioinspired nanocomposites (Figure 3). Compared with previous reports,[13,14] this study confirms that the covalent bonding would dramatically enhance the synergistic effect, providing a new strategy for further improving the mechanical properties through synergistic toughening.

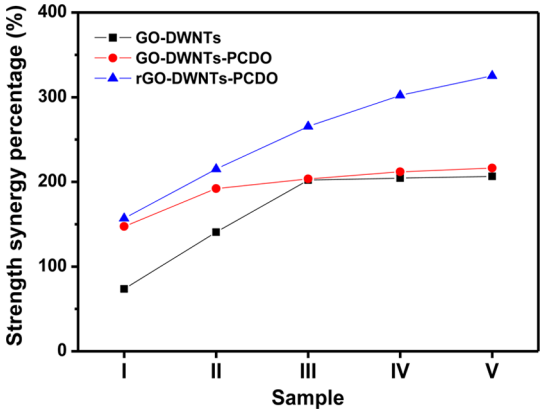

Figure 3. Synergy percentage (%) of tensile strength increases with GO contents in binary GO–DWNT hybrid materials and ternary GO–DWNT–PCDO nanocomposites.

In fact, this kind of synergistic effect also supplies the unique fatigue properties for ternary bioinspired nanocomposites besides static mechanical properties. The cyclic tensile loading tests were performed at a frequency of 1 Hz, and the stress ratio (R: minimum to maximum applied stress) was 0.1.[21] Figure 4a shows the maximum tensile stress (S) versus the number of cycles to failure (N) for pure GO film, GO–DWNT-V hybrid layered materials, and rGO–DWNT–PCDO-V ternary nanocomposites. The corresponding stress–strain fatigue curves are shown in Figure S9. It is obvious that the fatigue life of rGO–DWNT–PCDO-V ternary nanocomposites is almost 5 orders of magnitude higher than that of the GO–DWNT-V hybrid layered materials at the same stress level, further verifying the synergistic toughening effect from GO nanosheets and DWNTs. The 2D GO nanosheets suppress crack propagation by crack deflection and thus increase the fracture surface area during crack growth. The 1D DWNTs suppress crack propagation by crack bridging and a subsequent pull-out of DWNTs. These two crack suppression mechanisms act synergistically, increasing energy dissipation and prolonging fatigue life. The fracture morphology of GO–DWNT-V hybrid layered materials (Figure 4b) and rGO–DWNT–PCDO-V ternary nanocomposites (Figure 4c) after fatigue testing shows that DWNTs are curled much more than those of static mechanical testing, further conforming the 1D DWNT suppressing crack propagation by crack bridging.

The synergistic toughening of GO and DWNTs plus covalent bonding offers the advantage of integrated high strength, toughness, and electrically conductive rGO–DWNT–PCDO-V ternary nanocomposites compared with natural nacre and other binary GO-based nanocomposites with different interface interactions, such as hydrogen bonding (GO–PMMA,[22] rGO–PVA,[23] and rGO–SL[24]), ionic bonding (GO–Mg^{2+}, and GO–Ca^{2+}),[25] π–π conjugated interactions (rGO–PAPB[9]), and covalent bonding (GO–GA,[26] GO–borate,[10] PGO–PEI,[11]

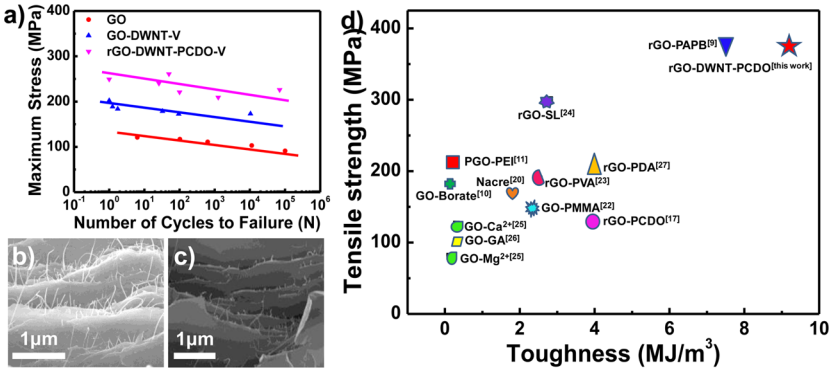

Figure 4. (a) Tensile fatigue testing of GO film, GO–DWNT hybrid layered materials, and rGO–DWNT–PCDO-V nanocomposites. The fracture morphology of (b) GO–DWNT-V hybrid layered materials and (c) rGO–DWNT–PCDO-V nanocomposite after fatigue testing. (d) Comparison of tensile strength and toughness of rGO–DWNT–PCDO-V nanocomposite with natural nacre and other binary GO-based nanocomposites.

rGO−PCDO,[17] and rGO−PDA[27]), as shown in Figure 4d. Detailed mechanical properties of natural nacre and GO-based nanocomposites are listed in Table S4. On the other hand, the mechanical properties of rGO−DWNT−PCDO-V ternary nanocomposites are much higher than our previous ternary nanocomposites of GO−MoS_2−TPU.[16] This is because the covalent bonding could further enlarge the synergistic effect. Furthermore, the electrical conductivity of rGO−DWNT−PCDO-V ternary bioninspired nanocomposites reaches as high as 394.0 ± 6.8 S/cm (Table S5), which is higher than that of the binary GO-based materials.[9,17,27] The use of rGO−DWNT−PCDO-V ternary nanocomposites as a conducting wire in a circuit is demonstrated in Figure S10. Compared with other binary nacre-inspired nanocomposites based on nanoclay,[28−34] this conductive graphene-based nacre-mimic nanocomposites show great potential applications in electrical-related areas, such as capacitors, lithium-ion batteries, *et al.* Meanwhile, this graphene-based nanocomposite film can also be further designed as functional materials through carefully choosing the initial assembly units, for example, the electrocatalysts.[35−37]

CONCLUSION

Natural nacre sets a "gold standard" for materials with integrated high strength and toughness. Inspired by the hierarchical micro/nanoscale structure of nacre, we have fabricated 2D rGO nanosheets and 1D DWNTs-based bioinspired nanocomposites that successfully integrate high strength and toughness. The synergistic effect from 2D rGO nanosheets and 1D DWNTs and covalent bonding resulted in extraordinary integrated mechanical properties. The tensile strength and toughness are 2.6 and 3.3 times that of pure reduced GO film, respectively. These integrated bioinspired nanocomposites also exhibit high electrical conductivity and excellent fatigue-resistant properties, which will enable new materials for a number of applications, such as aerospace, flexible energy devices, and artificial muscles. The synergistic building blocks with covalent bonding for constructing ternary bioinspired nanocomposites can serve as the basis of a novel strategy for the fabrication of integrated, high-performance, reduced graphene oxide (rGO)-based nanocomposites in the future.

METHODS

Materials. Crystalline graphite powder was purchased from Qingdao JingRiLai Graphite Co., Ltd. High-purity double-walled carbon nanotubes (DWNTs) with a diameter of about 1.8 nm were purchased from XianFeng NANO Co., Ltd. 10,12-Pentacosadiyn-1-ol (PCDO) was purchased from Tokyo Chemical Industry Co., Ltd., and 57 wt % hydroiodic acid (HI) was purchased from Sigma−Aldrich.

Fabrication of GO−DWNT Hybrid Layered Materials. Graphene oxide (GO) was prepared by the modified Hummers' method. The diameter of GO is 1.0−3.0 μm. A certain amount of GO nanosheets were dispersed in deionized water, followed by continuous stirring for 1 h and ultrasonication for 30 min. Then the homogeneous GO solution was obtained. The DWNT dispersion solution was slowly dropped into the GO solution under continuous ultrasonication. Finally, the mixture solution of GO/DWNTs was transferred into a tetrafluoroethylene container, which was placed into an oven with a temperature of 45 °C for 2 days. The GO−DWNT hybrid layered materials were obtained.

Fabrication of Ternary Bioinspired Nanocomposites. First, the GO−DWNT hybrid layered materials were immersed in a PCDO/THF solution. Subsequently, the PCDO-grafted GO−DWNT were treated under UV irradiation at a wavelength of 365 nm at the atmosphere of nitrogen. The final GO−DWNT−PCDO nanocomposites were rinsed, and then reduced by 57 wt % HI solution. Finally, the rGO−DWNT−PCDO nanocomposites were obtained after washing with deionized water and alcohol and drying.

Characterization. Mechanical properties were tested by a Shimadzu AGS-X Tester with gauge length of 5 mm and loading rate of 1 mm/min. All measurements were conducted at room temperature and all specimens were dried for 24 h at 45 °C before testing. The samples were cut into strips with the width of 3 mm and length of 10 mm, and the thickness of all samples were calculated by scanning electron microscopy (SEM). The Young's modulus of all samples was determined by the slope of the linear region of the stress−strain curves. The toughness was calculated by the area under the stress−strain curves. The mechanical properties for each sample are based on the average value of 3−5 specimens. Tensile fatigue tests were measured by InstronElectroPuls E1000 test facility with a frequency of 1 Hz. Scanning electron microscopy (SEM) images were obtained by Quanta 250 FEG and JSM-7500F. Transmission electron microscopy (TEM) images were obtained using an FEI Tecnai G20 instrument at 200 kV. The thermogravimetric analysis (TGA) was performed on NETZSCH STA449F3 under nitrogen with a temperature rising rate of 10 °C/min from room temperature to 800 °C. Fourier transform infrared spectroscopy (FTIR) were collected using a Thermo Nicolet Nexus470 FTIR instrument. All of the X-ray photoelectron spectroscopy (XPS) measurements were taken in an ESCALab220i-XL (ThermoScientific) using a monochromatic Al-Ka X-ray source. X-ray diffraction (XRD) was collected from Shimadzu LabX XRD-6000. The electrical conductivities of the ternary bioinspired nanocomposites were measured by a standard two-probe method using a source meter (Agilent E4980A).

Conflict of Interest: The authors declare no competing financial interest.

Acknowledgment. This work was supported by the Excellent Young Scientist Foundation of NSFC (51522301), the National Natural Science Foundation of China (21273017, 51103004), Program for New Century Excellent Talents in University (NCET-12-0034), Beijing Nova Program (Z121103002512020), Fok Ying-Tong Education Foundation (141045), Open Project of Beijing National Laboratory for Molecular Sciences, the 111 Project (B14009), Aeronautical Science Foundation of China (20145251035), State Key Laboratory for Modification of Chemical Fibers and Polymer Materials, Donghua University (LK1508), and the Fundamental Research Funds for the Central Universities (YWF-15-HHXY-001).

Supporting Information Available: The Supporting Information is available free of charge on the ACS Publications website at DOI: 10.1021/acsnano.5b05252.

Characterizations of bioinspired nanocomposites, such as TGA, SEM, XPS, fracture morphology, detailed tensile strength and toughness (PDF)

REFERENCES AND NOTES

1. Lee, C.; Wei, X.; Kysar, J. W.; Hone, J. Measurement of the Elastic Properties and Intrinsic Strength of Monolayer Graphene. *Science* **2008**, *321*, 385–388.
2. Novoselov, K. S.; Geim, A. K.; Morozov, S. V.; Jiang, D.; Zhang, Y.; Dubonos, S. V.; Grigorieva, I. V.; Firsov, A. A. Electric Field Effect in Atomically Thin Carbon Films. *Science* **2004**, *306*, 666–669.
3. Geim, A. K. Graphene: Status and Prospects. *Science* **2009**, *324*, 1530–1534.
4. Wegst, U. G. K.; Bai, H.; Saiz, E.; Tomsia, A. P.; Ritchie, R. O. Bioinspired Structural Materials. *Nat. Mater.* **2015**, *14*, 23–36.
5. Meyers, M. A.; McKittrick, J.; Chen, P.-Y. Structural Biological Materials: Critical Mechanics-Materials Connections. *Science* **2013**, *339*, 773–779.
6. Park, S.; Ruoff, R. S. Chemical Methods for the Production of Graphenes. *Nat. Nanotechnol.* **2009**, *4*, 217–224.
7. Cheng, Q.; Jiang, L.; Tang, Z. Bioinspired Layered Materials with Superior Mechanical Performance. *Acc. Chem. Res.* **2014**, *47*, 1256–1266.
8. Cheng, Q.; Duan, J.; Zhang, Q.; Jiang, L. Learning from Nature: Constructing Integrated Graphene-Based Artificial Nacre. *ACS Nano* **2015**, *9*, 2231–2234.
9. Zhang, M.; Huang, L.; Chen, J.; Li, C.; Shi, G. Ultratough, Ultrastrong, and Highly Conductive Graphene Films with Arbitrary Sizes. *Adv. Mater.* **2014**, *26*, 7588–7592.
10. An, Z.; Compton, O. C.; Putz, K. W.; Brinson, L. C.; Nguyen, S. T. Bio-Inspired Borate Cross-Linking in Ultra-Stiff Graphene Oxide Thin Films. *Adv. Mater.* **2011**, *23*, 3842–3846.
11. Tian, Y.; Cao, Y.; Wang, Y.; Yang, W.; Feng, J. Realizing Ultrahigh Modulus and High Strength of Macroscopic Graphene Oxide Papers Through Crosslinking of Mussel-Inspired Polymers. *Adv. Mater.* **2013**, *25*, 2980–2983.
12. Ritchie, R. O. The Conflicts between Strength and Toughness. *Nat. Mater.* **2011**, *10*, 817–822.
13. Prasad, K. E.; Das, B.; Maitra, U.; Ramamurty, U.; Rao, C. N. R. Extraordinary Synergy in the Mechanical Properties of Polymer Matrix Composites Reinforced with 2 Nanocarbons. *Proc. Natl. Acad. Sci. U. S. A.* **2009**, *106*, 13186–13189.
14. Shin, M. K.; Lee, B.; Kim, S. H.; Lee, J. A.; Spinks, G. M.; Gambhir, S.; Wallace, G. G.; Kozlov, M. E.; Baughman, R. H.; Kim, S. J. Synergistic Toughening of Composite Fibres by Self-Alignment of Reduced Graphene Oxide and Carbon Nanotubes. *Nat. Commun.* **2012**, *3*, 650.
15. Wang, J.; Cheng, Q.; Lin, L.; Jiang, L. Synergistic Toughening of Bioinspired Poly(vinyl alcohol)−Clay−Nanofibrillar Cellulose Artificial Nacre. *ACS Nano* **2014**, *8*, 2739–2745.
16. Wan, S.; Li, Y.; Peng, J.; Hu, H.; Cheng, Q.; Jiang, L. Synergistic Toughening of Graphene Oxide−Molybdenum Disulfide−Thermoplastic Polyurethane Ternary Artificial Nacre. *ACS Nano* **2015**, *9*, 708–714.
17. Cheng, Q.; Wu, M.; Li, M.; Jiang, L.; Tang, Z. Ultratough Artificial Nacre Based on Conjugated Cross-linked Graphene Oxide. *Angew. Chem., Int. Ed.* **2013**, *52*, 3750–3755.
18. Dikin, D. A.; Stankovich, S.; Zimney, E. J.; Piner, R. D.; Dommett, G. H. B.; Evmenenko, G.; Nguyen, S. T.; Ruoff, R. S. Preparation and Characterization of Graphene Oxide Paper. *Nature* **2007**, *448*, 457–460.
19. Pei, S.; Zhao, J.; Du, J.; Ren, W.; Cheng, H.-M. Direct Reduction of Graphene Oxide Films into Highly Conductive and Flexible Graphene Films by Hydrohalic Acids. *Carbon* **2010**, *48*, 4466–4474.
20. Jackson, A.; Vincent, J.; Turner, R. The Mechanical Design of Nacre. *Proc. R. Soc. London, Ser. B* **1988**, *234*, 415–440.
21. Yavari, F.; Rafiee, M. A.; Rafiee, J.; Yu, Z. Z.; Koratkar, N. Dramatic Increase in Fatigue Life in Hierarchical Graphene Composites. *ACS Appl. Mater. Interfaces* **2010**, *2*, 2738–2743.
22. Putz, K. W.; Compton, O. C.; Palmeri, M. J.; Nguyen, S. T.; Brinson, L. C. High-Nanofiller-Content Graphene Oxide-Polymer Nanocomposites *via* Vacuum-Assisted Self-Assembly. *Adv. Funct. Mater.* **2010**, *20*, 3322–3329.
23. Li, Y.-Q.; Yu, T.; Yang, T.-Y.; Zheng, L.-X.; Liao, K. Bio-Inspired Nacre-like Composite Films Based on Graphene with Superior Mechanical, Electrical, and Biocompatible Properties. *Adv. Mater.* **2012**, *24*, 3426–3431.
24. Hu, K.; Tolentino, L. S.; Kulkarni, D. D.; Ye, C.; Kumar, S.; Tsukruk, V. V. Written-in Conductive Patterns on Robust Graphene Oxide Biopaper by Electrochemical Microstamping. *Angew. Chem., Int. Ed.* **2013**, *52*, 13784–13788.
25. Park, S.; Lee, K. S.; Bozoklu, G.; Cai, W.; Nguyen, S. T.; Ruoff, R. S. Graphene oxide papers modified by divalent ions - Enhancing Mechanical Properties *via* Chemical Cross-Linking. *ACS Nano* **2008**, *2*, 572–578.
26. Gao, Y.; Liu, L.-Q.; Zu, S.-Z.; Peng, K.; Zhou, D.; Han, B.-H.; Zhang, Z. The Effect of Interlayer Adhesion on the Mechanical Behaviors of Macroscopic Graphene Oxide Papers. *ACS Nano* **2011**, *5*, 2134–2141.
27. Cui, W.; Li, M.; Liu, J.; Wang, B.; Zhang, C.; Jiang, L.; Cheng, Q. A Strong Integrated Strength and Toughness Artificial Nacre Based on Dopamine Cross-Linked Graphene Oxide. *ACS Nano* **2014**, *8*, 9511–9517.
28. Tang, Z.; Kotov, N. A.; Magonov, S.; Ozturk, B. Nanostructured Artificial Nacre. *Nat. Mater.* **2003**, *2*, 413–418.
29. Podsiadlo, P.; Kaushik, A. K.; Arruda, E. M.; Waas, A. M.; Shim, B. S.; Xu, J. D.; Nandivada, H.; Pumplin, B. G.; Lahann, J.; Ramamoorthy, A.; et al. Ultrastrong and Stiff Layered Polymer Nanocomposites. *Science* **2007**, *318*, 80–83.
30. Yao, H.-B.; Tan, Z.-H.; Fang, H.-Y.; Yu, S.-H. Artificial Nacre-like Bionanocomposite Films from the Self-Assembly of Chitosan−Montmorillonite Hybrid Building Blocks. *Angew. Chem., Int. Ed.* **2010**, *49*, 10127–10131.
31. Walther, A.; Bjurhager, I.; Malho, J.-M.; Ruokolainen, J.; Berglund, L.; Ikkala, O. Supramolecular Control of Stiffness and Strength in Lightweight High-Performance Nacre-Mimetic Paper with Fire-Shielding Properties. *Angew. Chem., Int. Ed.* **2010**, *49*, 6448–6453.
32. Walther, A.; Bjurhager, I.; Malho, J.-M.; Pere, J.; Ruokolainen, J.; Berglund, L. A.; Ikkala, O. Large-Area, Lightweight and Thick Biomimetic Composites with Superior Material Properties *via* Fast, Economic, and Green Pathways. *Nano Lett.* **2010**, *10*, 2742–2748.
33. Yao, H.-B.; Ge, J.; Mao, L.-B.; Yan, Y.-X.; Yu, S.-H. 25th Anniversary Article: Artificial Carbonate Nanocrystals and Layered Structural Nanocomposites Inspired by Nacre: Synthesis, Fabrication and Applications. *Adv. Mater.* **2014**, *26*, 163–188.
34. Das, P.; Malho, J. M.; Rahimi, K.; Schacher, F. H.; Wang, B. C.; Demco, D. E.; Walther, A. Nacre-mimetics with Synthetic Nanoclays up to Ultrahigh Aspect Ratios. *Nat. Commun.* **2015**, *6*, 6967.
35. Yin, H.; Tang, H.; Wang, D.; Gao, Y.; Tang, Z. Facile Synthesis of Surfactant-Free Au Cluster/Graphene Hybrids for High-Performance Oxygen Reduction Reaction. *ACS Nano* **2012**, *6*, 8288–8297.
36. Tang, H.; Yin, H.; Wang, J.; Yang, N.; Wang, D.; Tang, Z. Molecular Architecture of Cobalt Porphyrin Multilayers on Reduced Graphene Oxide Sheets for High-Performance Oxygen Reduction Reaction. *Angew. Chem., Int. Ed.* **2013**, *52*, 5585–5589.
37. Zhao, S.; Yin, H.; Du, L.; Yin, G.; Tang, Z.; Liu, S. Three Dimensional N-doped Graphene/PtRu Nanoparticle Hybrids as High Performance Anode for Direct Methanol Fuel Cells. *J. Mater. Chem. A* **2014**, *2*, 3719–3724.